ESCOLA UNIVERSITÁRIA VASCO DA GAMA

MESTRADO INTEGRADO EM MEDICINA VETERINÁRIA

MAGNETIC RESONANCE IMAGING AND ITS APPLICABILITY IN VETERINARY CARDIOLOGY

José Manuel de Seiça Ferreira

Coimbra, Fevereiro de 2016

ESCOLA UNIVERSITÁRIA VASCO DA GAMA

MESTRADO INTEGRADO EM MEDICINA VETERINÁRIA

MAGNETIC RESONANCE IMAGING AND ITS APPLICABILITY IN VETERINARY CARDIOLOGY

Coimbra, Fevereiro de 2016

José Manuel de Seiça Ferreira

Aluno do Mestrado Integrado em Medicina Veterinária

Orientador Interno

Professora Doutora Maria João Nobre de Matos Pereira Vieira

Orientador Externo

Dr. João Manuel Pimenta Ferreira de Oliveira

Médico Veterinário

Dissertação do estágio curricular dos ciclos de estudo conducentes ao Grau de Mestre em Medicina Veterinária da EUVG

Abstract

Magnetic Resonance Imaging (MRI) is a technique whereby images are created by the manipulation of hydrogen atoms in magnetic fields; it is based on the principle of nuclear magnetic resonance (MR), which is non-invasive and non-ionising (Constantine, Shan, Flamm, & Sivananthan, 2004). Cardiac Magnetic Resonance Imaging (CMRI) uses the same principle: application of magnetic-field gradients that are adjusted to highlight desired tissue characteristics, producing a variety of sequences that allow detection of cardiac tissue and blood, and consequently anatomical and/or physiological abnormalities (Jeudy & White, 2008; Constantine *et al.*, 2004). Basic pulse sequences used in CMRI are spin-echo and gradient-echo sequences, or their faster hybrids dark- or black-blood and bright-blood respectively (Constantine *et al.*, 2004).

CMRI is rapidly developing and is now an important diagnostic tool in human clinical cardiology (Gilbert, McConnell, Holden, Sivananthan, & Dukes-McEwan, 2010). In veterinary medicine the use of CMRI is still sporadic; its limitations in this field include the need for general anaesthesia, the cost and availability of the equipment, the steep learning curve to obtain and analyse the images, and the time needed to manually trace endocardial borders if semi-automated analysis is not available (MacDonald, Kittleson, Garcia-Nolen, Larson, & Wisner, 2006). CMRI was considered to be the reference method in many veterinary studies (Eskofier, Wefstaedt, Beyerbach, Nolte, & Hungerbuhler, 2015; Fattal *et al.*, 2015; Sargent *et al.*, 2015). Still, not many studies have been published or made available in this field. It is therefore essential to fully ascertain the clinical applications, advantages and limitations of CMRI in veterinary medicine. The aim of this review is to identify the potential applications of CMRI from a clinical point of view and compare it with echocardiography, which is still the gold standard in veterinary cardiology. We describe the principles and technique of MRI in small animal cardiology, and the diseases in which CMRI could be an important tool for diagnosis and prognosis.

Key-words: Magnetic Resonance Imaging; Cardiac Magnetic Resonance Imaging; veterinary cardiology; dogs; cats

List of contents

Introduction 1

1. Principles and Technique of Magnetic Resonance Imaging 2

1.1. Magnetic Resonance Imaging physics 2

1.2. Sequences used in Cardiac Magnetic Resonance Imaging 3

1.2.1. Spin-echo pulse sequence: Black-Blood 4

1.2.2. Gradient-echo pulse sequence: Bright-Blood 4

1.3. Performance of a Cardiac Magnetic Resonance Imaging examination under general anaesthesia 5

1.4. Contrast agents used in Magnetic Resonance Imaging 6

2. Cardiac Magnetic Resonance Imaging in veterinary medicine 8

2.1. Echocardiography *vs* Magnetic Resonance Imaging 8

2.2. Morphology and function 8

2.3. Left ventricular myocardial mass, chamber volume and haemodynamic 12

2.4. Valvular heart disease 13

2.5. Cardiomyopathies 14

2.5.1. Hypertrophic cardiomyopathy 14

2.5.2. Dilated cardiomyopathy 15

2.5.3. Arrhythmogenic Right Ventricular Cardiomyopathy 15

2.5.4. Myocarditis and myocardial viability 16

2.6. Congenital heart disease 17

2.7. Ischemic disease 18

2.8. Pericardial disease 18

2.9. Other applications 19

3. Specific difficulties with transposition of human Cardiac Magnetic Resonance Imaging to veterinary cardiology 19

4. Cardiac Magnetic Resonance Imaging studies in cats and dogs – experimental or clinical? 19

5. Future perspectives 20

Conclusion 21

References 22

List of figures

Figure 1: Representation of the application of radiofrequency (RF) and the transversal magnetisation. 3

Figure 2: Representation of the deflected protons returning to its original position. 3

Figure 3: Comparison between black-blood (left) and bright-blood (right) axial images of the human hearth. Adapted from: Jeudy and White (2008). 5

Figure 4: Positioning of the cat for CMRI examination. Adapted from: MacDonald, Kittleson, *et al.* (2005). 6

Figure 5: Late gadolinium enhancement imaging of a rat heart with myocarditis in short-axis (left) and four-chamber (right) views. Image courtesy of Rinkevich-Shop *et al.* (2013). 7

Figure 6: Short axis view of the left ventricle: end diastolic (left) and end systolic (right). Adapted from: Drees, Johnson, Stepien, Munoz Del Rio, Saunders, *et al.* (2015) 10

Figure 7: End systolic (left) and end diastolic (right) three-chamber view. Adapted from: Drees, Johnson, Stepien, Munoz Del Rio, Saunders, *et al.* (2015). 11

Figure 8: Approximate four-chamber view (left) and transverse plan (right). Adapted from: Drees, Johnson, Stepien, Munoz Del Rio, Saunders, *et al.* (2015). 11

Figure 9: Pathological changes in boxer dogs with ARVC. Source: Basso *et al.* (2004). 16

Figure 10: Late gadolinium enhanced (LGE) distribution in left ventricle (LV) of rats with myocarditis. Image courtesy of Rinkevich-Shop *et al.* (2013). 17

List of tables

Table 1: Left ventricular planar measurements generated from echocardiographic exams obtained in 10 awaken dogs, as well as CMRI with two different anaesthetic protocols. Adapted from: Drees, Johnson, Stepien, Munoz Del Rio, and Francois (2015)..... 9

Table 2: Right ventricular function variables comparing CMRI, computed tomography and three-dimensional echocardiography in dogs. Adapted from: Kim *et al.* (2013), Sieslack *et al.* (2014) and Meyer *et al.* (2013) 12

List of abbreviations

3DE – three-dimensional echocardiography

Ao – aorta

Ao annulus 3ch – aortic annulus measured on three-chamber view

Ao/PA ratio – aorta to pulmonary artery ratio

ARVC – arrhythmogenic right ventricular cardiomyopathy

CCT – cardiac computed tomography

CMRI – cardiac magnetic resonance imaging

ECG – electrocardiogram

EDV – end-diastolic volume

EF – ejection fraction

ESV – end-systolic volume

IVS – interventricular septum

IVSd – diastolic interventricular septal

IVSs – systolic interventricular septal

LA – left atrium

LA diam 3ch – left atrial diameter measured on three-chamber view

LA/Ao ratio – left atrium to aorta ratio

LGE – late gadolinium enhanced

LPA – left pulmonary artery

LV – left ventricle

LVID – left ventricular internal diameter

LVIDd – diastolic left ventricular internal diameter

LVIDs – systolic left ventricular internal diameter

LVPW – left ventricular posterior wall

LVPWd – diastolic left ventricular posterior wall

LVPWs – systolic left ventricular posterior wall

Mitral annulus 3ch – mitral annulus measured on three-chamber view

Mitral annulus 4ch – mitral annulus measured on four-chamber view

MPA – main pulmonary artery

MRI – magnetic resonance imaging

prox Ao – proximal aorta measured on transverse plane

RF – radiofrequency

RPA – right pulmonary artery

RV – right ventricle

SV – stroke volume

Introduction

MRI has become recognized as a useful referral diagnostic method in veterinary medicine, and is widely used in small animal brain and spinal diseases (Gavin, 2011; Gilbert *et al.*, 2010), aural, nasal and orbital disorders, planning soft tissue surgery, oncology and small animal and equine orthopaedics (Gilbert *et al.*, 2010). The use of MRI in these subjects has grown due to its unparalleled capability to image soft tissue structures (Gilbert *et al.*, 2010) to a much better degree than other modalities (Constantine *et al.*, 2004).

During the past decade, the application of MRI to cardiology has provided new insights in the investigation of cardiovascular diseases. With technological advancements, we can now rapidly acquire large imaging datasets that are essential for imaging the heart (Constantine *et al.*, 2004). This has been successfully applied to human cardiology where, despite the inherent difficulties in imaging a moving and contractile structure, CMRI has become the optimal technique for the morphological assessment and quantification of ventricular function (Gilbert *et al.*, 2010; Vallee, Ivancevic, Nguyen, Morel, & Jaconi, 2004). It is also a clinically important technique for the assessment of cardiac structure, function, perfusion, and myocardial viability (Constantine *et al.*, 2004; Vallee *et al.*, 2004). In veterinary medicine, CMRI is considered to be the gold standard technique for right ventricular volumetric measurement (Sieslack, Dziallas, Nolte, Wefstaedt, & Hungerbuhler, 2014) because of its high temporal and spatial resolution and its detailed soft tissue contrast, resulting in high accuracy and reproducibility of the measurements. CMRI has also been considered to be a reference method in many studies when compared with real-time two-dimensional and three-dimensional echocardiography; in dogs it was been used to the quantification of left ventricular volume (Eskofier *et al.*, 2015; Sieslack *et al.*, 2014), and function in anaesthetized dogs (Eskofier *et al.*, 2015); to quantify right ventricular volume (Sieslack *et al.*, 2014); to evaluate mitral regurgitation (Sargent *et al.*, 2015); to study cardiac morphology and function in Boxer with arrhythmogenic right ventricular cardiomyopathy (ARVC) (Baumwart, Meurs, & Raman, 2009); to differentiate neoplastic and non-neoplastic pericardial effusion (Boddy *et al.*, 2011); and in cats to study hypertrophic cardiomyopathy (MacDonald, Wisner, *et al.*, 2005; Sugimoto, Fujii, Sunahara, & Aoki, 2015).

CMRI is a promising diagnostic tool for the majority of cardiac pathologies. However, some studies are needed to compare the measurements and values obtained by CMRI and echocardiography to standardize the technique and establish reference values by animal breed, weight and age. It is essential to fully ascertain the clinical applications, advantages and limitations of CMRI in veterinary medicine in comparison to the more widespread and proven diagnostic tool that is echocardiography.

1. Principles and Technique of Magnetic Resonance Imaging

MRI is a non-invasive and non-ionising radiation technique based on the principle of nuclear magnetic resonance, and has intrinsic attributes well suited for cardiac imaging as being a tomographic technique that can acquire images in virtually any orientation (Constantine *et al.*, 2004).

1.1. Magnetic Resonance Imaging physics

The acquisition of MRI images depends on protons; images are derived from signals produced by the protons (hydrogen nuclei), which are mainly attached to water molecules. The proton behaves like a small magnet that spins when placed in a magnetic field; this produces a small magnetic field that can align with a superconducting magnet of a larger magnetic field (Constantine *et al.*, 2004; Jeudy & White, 2008). Protons will align with the primary magnetic field, both parallel and antiparallel to its direction; in addition, a spatially applied field generates slightly different spins along a gradient. A radiofrequency pulse can then be applied in such a way that only protons spinning at the same frequency as the radiofrequency pulse will capture the radiofrequency energy and change the direction of their magnetization (figure 1) (Jeudy & White, 2008). The magnetization of these protons is then momentarily deflected away from the direction of the vector of the superconducting magnet. After the radiofrequency pulse ceases, these deflected protons relax back towards their original position (relaxation*)* releasing energy in the form of a radiofrequency signal (figure 2). This signal is captured by a radiofrequency receiver coil and forms the basis for images obtained on MRI (Jeudy & White, 2008). The return of the net magnetisation vector to equilibrium has two components: the vector component parallel to the main field returns to equilibrium by interacting with surrounding molecules which is a relatively slow process and is known as T1 relaxation (longitudinal). The vector component transverse to the field is more rapid to decline, resulting from the interaction between individual spins, and is termed T2 relaxation (transverse) (Constantine *et al.*, 2004). A series of radiofrequency pulses of varying duration or strength and application of magnetic-field gradients that are adjusted to highlight desired tissue characteristics produce a variety of sequences that are applicable to CMRI (Constantine *et al.*, 2004; Jeudy & White, 2008).

Cardiac and respiratory motion artifacts can be overcome in human awake subjects by electrocardiography-gating (using electrocardiogram (ECG) signal to synchronizing data acquisition with specific phases of the cardiac cycle to eliminate artifacts due to cardiac motion (Gilbert *et al.*, 2010; Mai, Badea, Wheeler, Hedlund, & Johnson, 2005)) and breath-hold navigation; this allowed for real-time techniques to be developed and refined to synchronise data acquisition and keep artifacts to a minimum or eliminate them, thus allowing for clear and precise images of morphology and function. However when using ECG-gating, cardiac dysrhythmias can significantly interfere with synchronised data acquisition (Constantine, Shan *et al.* 2004).

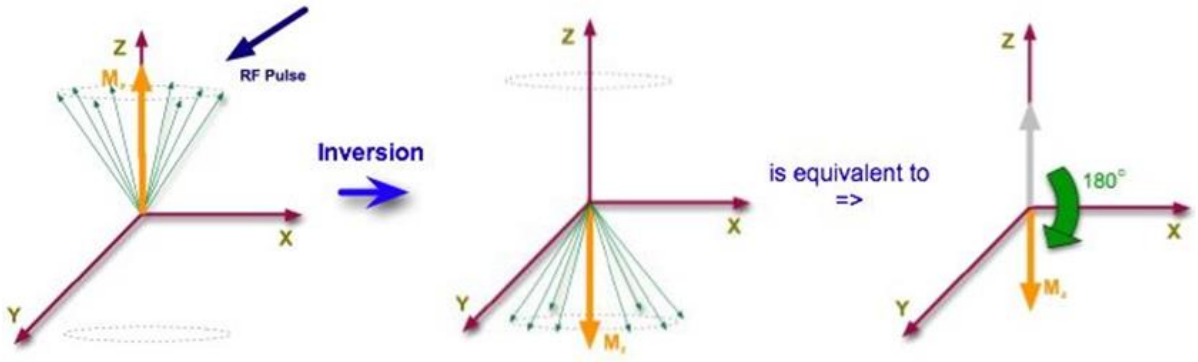

Figure 1: Representation of the application of radiofrequency (RF) and the transversal magnetisation. The application of a RF pulse in such a way that only protons spinning at the same frequency as the RF pulse will capture the radiofrequency energy and change the direction of their magnetization.
Source: https://upload.wikimedia.org/wikibooks/en/9/97/InvRecov3.jpg; acessed on 13.02.2016

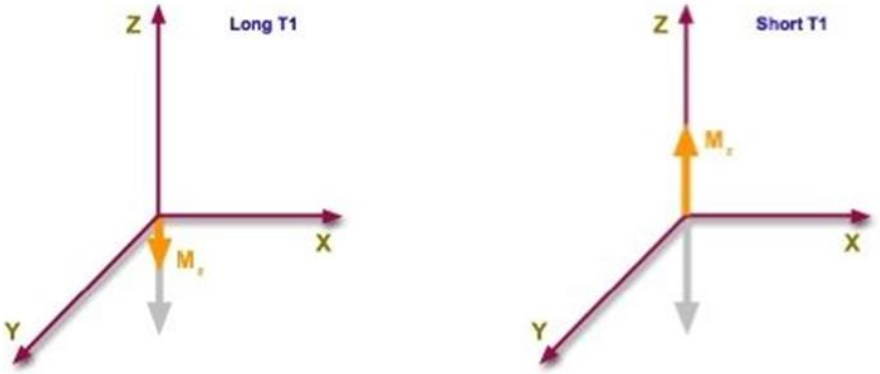

Figure 2: Representation of the deflected protons returning to its original position.
Source: https://upload.wikimedia.org/wikibooks/en/2/27/InvRecov6_1.jpg; **acessed on 13.02.2016**

1.2. Sequences used in Cardiac Magnetic Resonance Imaging

Most common pulse sequences used in CMRI are spin-echo and gradient-echo, or their faster hybrids dark- or black-blood and bright-blood respectively (Constantine *et al.*, 2004). Spin-echo sequences are chosen for the assessment of morphology, and flowing blood appears black (figure 3); on the other hand gradient-echo sequences are used in the assessment of valvular lesions, shunts, great vessels, ventricular function and wall-motion characteristics (Constantine *et al.*, 2004; Gilbert *et al.*, 2010). Gradient-echo sequences have fairly low soft-tissue contrast compared with spin-echo sequences, in gradient-echo the flowing blood is represented by high signal intensity and turbulence as areas of signal void (figure 3) (Constantine *et al.*, 2004).

1.2.1. Spin-echo pulse sequence: Black-Blood

Black-blood imaging was conventionally done with multi-slice T1-weighted spin-echo sequences; this sequence frequently provides excellent high quality anatomic images of cardiac chambers, great vessels and pericardium, and is relatively unaffected by metallic artifacts. These sequences are of uttermost importance when precise anatomic detail is necessary (Jeudy & White, 2008) such as in the assessment of scar tissue formed in chronic infarct (Kali *et al.*, 2014; Thajudeen *et al.*, 2015).

Recently, T1-weighted spin-echo imaging sequences have largely been supplanted by echo-train imaging with double inversion sequences because of its rapidity, this approach can be applied in a single slice per breath-hold fashion or images of the entire heart can be obtained in a single breath hold using a single-shot strategy (Jeudy & White, 2008), on the other hand fast T2-weighted images are used occasionally, especially for patients with cardiac masses or pericardial disease (Boddy *et al.*, 2011; Jeudy & White, 2008). The major disadvantage of this kind of sequences is the long imaging time of several minutes and the associated motion artifact that may occur (Jeudy & White, 2008).

1.2.2. Gradient-echo pulse sequence: Bright-Blood

Gradient-echo techniques are turbulence sensitive, and thus can be employed to detect areas of turbulent flow due to stenosis or regurgitation of blood flow around the lesions, as well as to explore the pattern of flow in shunts and vessels, and in the assessment of ventricular wall-motion (Constantine *et al.*, 2004; Jeudy & White, 2008); turbulent blood appears black in these techniques, while laminar flow appears bright (Gilbert *et al.*, 2010). The extent of stenosis or regurgitation can be quantified using velocity-encoded sequences (Jeudy & White, 2008). Using phase encoding velocity maps, flow volumes, and flow velocity, may then be quantified across valves or shunts (Constantine *et al.*, 2004; Gilbert *et al.*, 2010).Typically bright-blood images are placed in a cine-loop; this format allows good visualization of cardiac motion at a single level in any plane during the cardiac cycle, and is essential to determine cardiac ejection fraction and to assess wall motion (Jeudy & White, 2008). Important disadvantages of gradient-echo techniques include high sensitivity to inhomogeneity in the magnetic field, images' propensity to artifacts from metal (Jeudy & White, 2008) and less contrast between blood and soft tissue being provide by these sequences (Constantine *et al.*, 2004).

Bright-blood sequences have increasingly become the backbone of human CMRI. Initially, bright-blood imaging was performed with a spoiled gradient-echo sequence and a single view was obtained per cardiac cycle, requiring an acquisition time of several minutes; later on, further development of gradient-echo techniques allowed for the acquisition in a single breath-hold. Spoiled gradient techniques are also limited by relatively poor endomyocardial detail (Jeudy & White, 2008). Using bright-blood sequences allows for global and regional function to be evaluated, and parameters like ejection fraction or wall thickness being reproducibly extracted based on the high contrast between blood and the myocardium (Vallee *et al.*, 2004). The current bright-blood sequence benchmark is steady-state free precession, which allows more reliable distinction of the endomyocardial border,

better contrast, and less sensitivity to slow flow. When compared with earlier techniques this new method employs a very short reaction time and is thus substantially faster than spoiled gradient echo techniques. The similarity between spoiled gradient sequences and steady-state free precession sequences is that they can be performed in a single breath-hold but with improved temporal resolution; such fast imaging is critical to obtain physiologic information regarding myocardial function (Jeudy & White, 2008). Steady-state free precession sequences can also be used to obtain non-gated free-breathing images, which may be advantageous in patients who have difficulty breath-holding or in individuals with arrhythmias that make gating difficult (Jeudy & White, 2008; Vallee *et al.*, 2004).

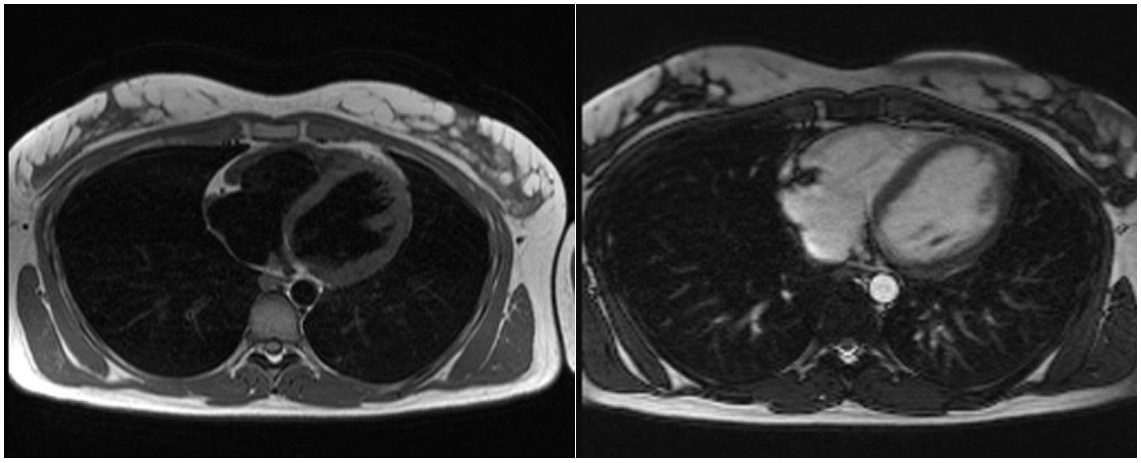

Figure 3: Comparison between black-blood (left) and bright-blood (right) axial images of the human hearth. In black-blood (left) the flowing blood appears black and in bright-blood (right) the flowing blood is represented by high signal intensity and turbulence as areas of signal void. Adapted from: Jeudy and White (2008).

1.3. Performance of a Cardiac Magnetic Resonance Imaging examination under general anaesthesia

In human subjects, there is no need for general anaesthesia for CMRI examinations as humans remain calm within the noisy and confined MRI environment, and can be instructed to hold their breath (Gilbert *et al.*, 2010). This is not the case for infants and small children, who are routinely imaged under general anaesthesia or sedation (Jeudy & White, 2008), nor it is for animals, for whom general anaesthesia or sedation is always required (Gilbert *et al.*, 2010; Sharpley *et al.*, 2009). To perform the examination, the animal is intubated with a cuffed endotracheal tube, placed on dorsal recumbence with the hind limbs extended (Drees, Johnson, Stepien, Munoz Del Rio, Saunders, *et al.*, 2015), electrodes are placed (MRI-compatible electrocardiography) and the appropriate surface coil is positioned on the thorax at the level of the heart (Gilbert *et al.*, 2010) (figure 4). The animal kept anaesthetised with controlled rate infusion of propofol (MacDonald, Kittleson, *et al.*, 2005) or on volatile anaesthesia and 100% oxygen with positive pressure ventilation (Drees, Johnson, Stepien,

Munoz Del Rio, Saunders, *et al.*, 2015; MacDonald *et al.*, 2006; Sharpley *et al.*, 2009). The imaging can then be carried out during apnoea following hyperventilation (Gilbert *et al.*, 2010).

General anaesthesia in CMRI cases is often complicated by the presence of cardiac disease, and many animals will be geriatric, so the anaesthetic complexity is higher. In addition, the CMRI room environment imposes restrictions on the anaesthetic and monitoring equipment which must be safe for use near the magnet (i.e. must not contain ferrous metals) (Gilbert *et al.*, 2010). In a retrospective study of infant and small children, Odegard *et al.* (2004), listed the difficulties in monitoring, and enumerated the anaesthetic protocols to be adopted. They concluded that CMRI could be performed safely under general anaesthesia in children with congenital cardiac disease despite the complexity and pathophysiology of many of the defects, the frequent breath-holding for image acquisition and the CMRI environment. Another important fact of this study was the fact that one child had moderate to severe left ventricular dysfunction and another child had a body mass of 1,3 kg, similarly to cats or small dogs (Gilbert *et al.*, 2010).

Figure 4: Positioning of the cat for CMRI examination. Adapted from: MacDonald, Kittleson, *et al.* (2005).

1.4. Contrast agents used in Magnetic Resonance Imaging

Gadolinium-based MRI contrast agents are by far the most commonly used; there are some gadolinium-based contrast agents commercialized for clinical use, primarily indicated for central nervous system, vasculature, and whole body exams. Typically, gadolinium-based contrast agents lower the T1 *in vivo* to create a higher signal in T1-weighted MRI scans (Hao *et al.*, 2012). Administration of gadolinium contrast is also useful for tissue characterization and improved mass delineation, by means of differential enhancement due to variation in tumour vascularity and altered

capillary permeability at both dynamic and delayed imaging (Sparrow, Kurian, Jones, & Sivananthan, 2005). These agents for use in CMRI are safer than the iodinated ones used in radiography: the majority of gadolinium agents are not nephrotoxic and have a lower rate of serious adverse events compared to iodinated contrast agents used on radiography contrast. Even so, they still present some risk, like nephrogenic toxicity and fibrosis (Constantine *et al.*, 2004; Hao *et al.*, 2012).

In humans histological studies comparing late gadolinium images, macroscopic slices, and histologic samples showed concordance between the regions of enhancement and collagen (Moon *et al.*, 2004). Rinkevich-Shop *et al.* (2013) did the same comparison in rats in a non-invasive assessment of experimental autoimmune myocarditis, also showing concordance. These results support the idea that late gadolinium enhancement in CMRI provides a means of quantifying fibrosis *in vivo* (figure 5).

In a study by Moon *et al.* (2004) to identify the histological basis of late gadolinium enhancement CMRI in hypertrophic cardiomyopathy, a dose of 0.1 mmol/kg of gadolinium-diethylenetriamine pentaacetic acid as used, and the images acquired after 10 minutes, whereas in a case report of patent ductus arteriosus in a dog, done by Louvet, Duconseille, and Lazard (2010), a dose of 0,2 mmol/kg was used.

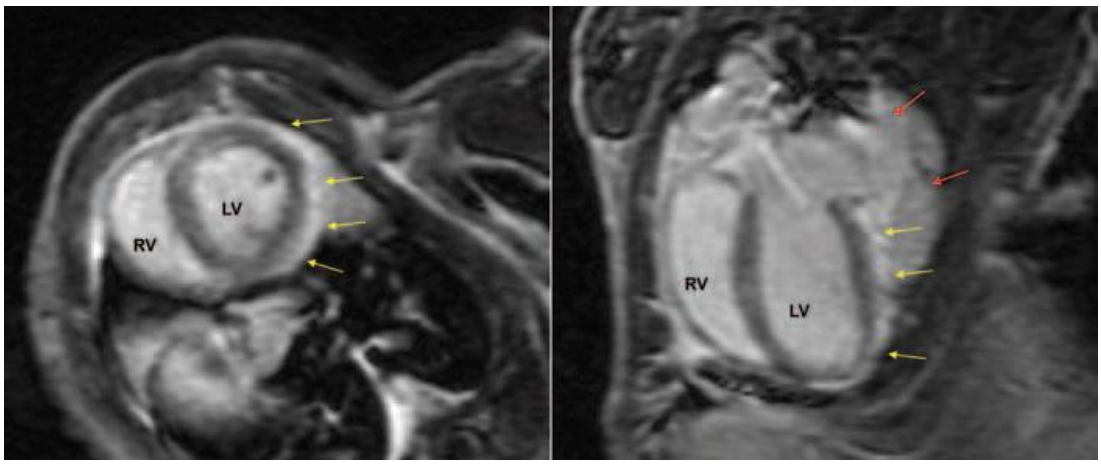

Figure 5: Late gadolinium enhancement imaging of a rat heart with myocarditis in short-axis (left) and four-chamber (right) views[1]. Image courtesy of Rinkevich-Shop *et al.* (2013).

[1] This figure shows typical epicardial late gadolinium enhancement (hyper-intense strip, yellow arrows), while sparing the sub-endocardium. Pericardial effusion is marked by red arrows.
Legend: LV, left ventricle; and RV, right ventricle.

2. Cardiac Magnetic Resonance Imaging in veterinary medicine

2.1. Echocardiography *vs* Magnetic Resonance Imaging

Non-invasive imaging methods like echocardiography and MRI are very valuable in longitudinal follow-up studies of cardiac function in small animals (Amundsen *et al.*, 2011; Jeudy & White, 2008) and pericardial morphology, and is an excellent technique to use in left ventricle functional variables assessment (Jeudy & White, 2008). Regarding the evaluation of cardiomyopathies, CMRI is a reference standard imaging technique due to the accurate measurement of cardiac volumes and mass (Puntmann *et al.*, 2013). In clinical routine, however, echocardiography is the standard first-line technique mainly due to its convenience and straightforwardness (Asferg, Usinger, Kristensen, & Abdulla, 2012; Puntmann *et al.*, 2013).

CMRI is more accurate than echocardiography in providing measurements of cardiac chamber volumes (Rinkevich-Shop *et al.*, 2013), dimensions and wall thickness (Puntmann *et al.*, 2013), regional and global function, perfusion, and tissue characterization, with high reproducibility (MacDonald, Kittleson, *et al.*, 2005; Rinkevich-Shop *et al.*, 2013). CMRI can also quantify functional abnormalities and characterize morphological changes such as fatty infiltration of the right ventricle and an excellent tool to demonstrate complex vascular anatomy, something that is limited in echocardiography because of its narrow acoustic window (Baumwart *et al.*, 2009; Lopez-Alvarez *et al.*, 2011; MacDonald, Kittleson, *et al.*, 2005). It is also more accurate and reliable in the measurement of the right heart, as shown by Shors and colleagues (2004) with a close agreement between right ventricular mass measurements at MRI and those observed at necropsy.

Echocardiography is consistently used to assess mitral regurgitation severity but measures of mitral regurgitation in dogs have not been compared with other quantitative methods (Sargent *et al.*, 2015). However, Kim *et al.* (2013) suggest that it is feasible to use contrast echocardiography in dogs in order to obtain left ventricular volume measurements in agreement with CMRI values, suggesting that echocardiography can still be used instead of CMRI as a diagnostic tool for certain pathologies. Still, three-dimensional echocardiography underestimates true left ventricles volumes and ejection fraction and has a substantial degree of variance, especially in patients with poor acoustic windows or large ventricles (Dorosz, Lezotte, Weitzenkamp, Allen, & Salcedo, 2012), even so this still the most widespread diagnosis tool in cardiology.

2.2. Morphology and function

A variety of canine congenital and acquired heart diseases may disturb hemodynamic balance and lead to volume overload and regurgitation with possible effects such as pulmonary oedema, ascites, or sudden death from heart failure (Meyer *et al.*, 2013). High-frequency echocardiography tends to under-estimate left ventricular diameters in end-diastole, but not in end-systole, when compared to CMRI (Amundsen *et al.*, 2011; Mor-Avi *et al.*, 2008); in end-systole high-frequency echocardiography

also under-estimates wall thickness in the posterior wall, while there seems to be no difference in the anterior wall (Amundsen *et al.*, 2011) (table 1).

Table 1: Left ventricular planar measurements generated from echocardiographic exams obtained in 10 awaken dogs, as well as CMRI with two different anaesthetic protocols[2]. Adapted from: Drees, Johnson, Stepien, Munoz Del Rio, and Francois (2015).

Variable	Echocardiography	Magnetic Resonance Imaging	
		Protocol A	Protocol B
IVSd (cm)	0.76 (0.66-0.88)	0.79 (0.66-1.02)	0.77 (0.59-0.98)
IVSs (cm)	1.06 (0.95-1.2)	0.94 (0.66-1.47)	0.77 (0.44-1.04)
LVIDd (cm)	3.25 (2.79-3.63)	3.19 (2.97-3.45)	3.41 (2.84-3.63)
LVIDs (cm)	2.15 (1.67-2.45)	2.6 (2.04-2.96)	2.67 (2.23-3.07)
LVPWd (cm)	0.68 (0.53-0.79)	0.76 (0.52-0.94)	0.73 (0.7-0.94)
LVPWs (cm)	1.03 (0.85-1.17)	1.04 (0.46-1.25)	0.92 (0.65-1.22)
LA diam 3ch (cm)	2.21 (1.92-2.49)	2.8 (2.10-2.92)	2.72 (2.412.99)
Mitral annulus 3ch (cm)	-	2.02 (1.71-2.34)	1.94 (1.83-2.20)
Ao annulus 3ch (%)	1.71 (1.55-1.97)	1.17 (0.94-1347)	1.18 (1.04-1.34)
LA/Ao ratio	1.27 (1.18-1.49)	2.41 (1.93-3.04)	2.35 (1.8-2.64)
Mitral annulus 4ch (cm)	-	2.13 (1.69-2.23)	2.04 (1.8-2.34)
prox Ao (cm)	-	1.28 (1.07-1.6)	1.32 (1.18-1.56)
MPA (cm)	1.6 (1.5-1.8)	1.23 (1.11-1.24)	1.3 (1.12-1.56)
Ao/PA ratio	0.99 (0.86-1.31)	1.03 (0.96-1.22)	1.09 (0.98-1.19)

[2] All standard echocardiography studies were performed in awaken dogs. For CMRI all dogs were induced with propofol (2-6 mg/kg, intravenous) and maintained with isoflurane-oxygen mixture with an end-tidal concentration of 1-2%. Protocol A used fentanyl 5 µg/kg bolus for premedication followed by 10 µg/kg/h continuous rate infusion and midazolam 0.2 mg/kg bolus followed by 0.2 mg/kg/h constant rate infusion. Protocol B used dexmedetomedine 1–2 µg/kg bolus for premedication and 1–2 µg/kg/h constant rate infusion.

Legend: IVSd, diastolic interventricular septal thickness; IVSs, systolic interventricular septal thickness; LVIDd, diastolic left ventricular internal diameter, measured just proximal to the papillary muscles; LVIDs, systolic left ventricular internal diameter, measured just proximal to the papillary muscles; LVPWd, diastolic left ventricular posterior wall thickness; LVPWs, systolic left ventricular posterior wall thickness; LA diam 3ch, left atrial diameter measured on three-chamber view; Mitral annulus 3ch, mitral annulus measured on approximated three-chamber view; Ao annulus 3ch, aortic annulus measured on three-chamber view; LA/Ao ratio, left atrium to aorta ratio; Mitral annulus 4ch, mitral annulus measured on four-chamber view; prox Ao, proximal aorta measured on transverse plane; MPA, main pulmonary artery transverse plane; Ao/PA ratio, aorta to pulmonary artery ratio.

Some of the observed discrepancies (table 1) could have been caused by different visualization of the endocardial trabeculations in the two methods. In echocardiography, the *trabeculae* are well visualized because of the difference in their echogenicity in relation to blood. CMRI using a bright-blood sequence likely leads to the disappearance of the *trabeculae* in end-diastole when the trabecular layer is filled with blood. In end-systole, the *trabeculae* will be compressed and squeeze out the blood, explaining why there was no difference in end-systole (Mor-Avi *et al.*, 2008).

In veterinary cardiology, low-field magnetic resonance imaging of the heart can be useful, complementing the diagnostic information obtained by echocardiography (Garcia-Rodriguez *et al.*, 2009). Nevertheless, in human medicine cross-sectional imaging of the heart using MRI has been shown to be superior for the evaluation of cardiac morphology and systolic function, when compared to echocardiography (Drees, Johnson, Stepien, Munoz Del Rio, Saunders, *et al.*, 2015). The clinical importance of CMRI in veterinary medicine is well established with regard to morphological assessment of cardiac anomalies and great vessels. This role is partly attributed to the large field of view of CMRI, its unlimited scanning planes, and good contrast between tissue and blood. In addition, CMRI is a precise and highly reproducible method for measurement of right and left ventricular mass (Constantine *et al.*, 2004), function, and monitor pulmonary haemodynamic in patients with pulmonary hypertension (Roldan-Alzate *et al.*, 2014) (figures 6 to 8).

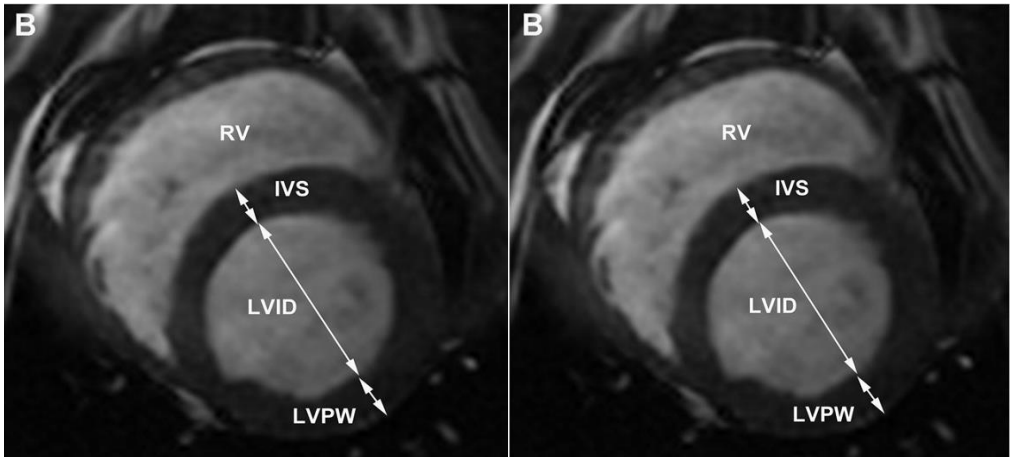

Figure 6: Short axis view of the left ventricle: end diastolic (left) and end systolic (right)[3]. Adapted from: Drees, Johnson, Stepien, Munoz Del Rio, Saunders, *et al.* (2015)

[3] This figure shows measurements of interventricular septum (IVS) and left ventricular posterior wall (LVPW) thickness and left ventricular internal diameter (LVID).

Legend: RV, right ventricle

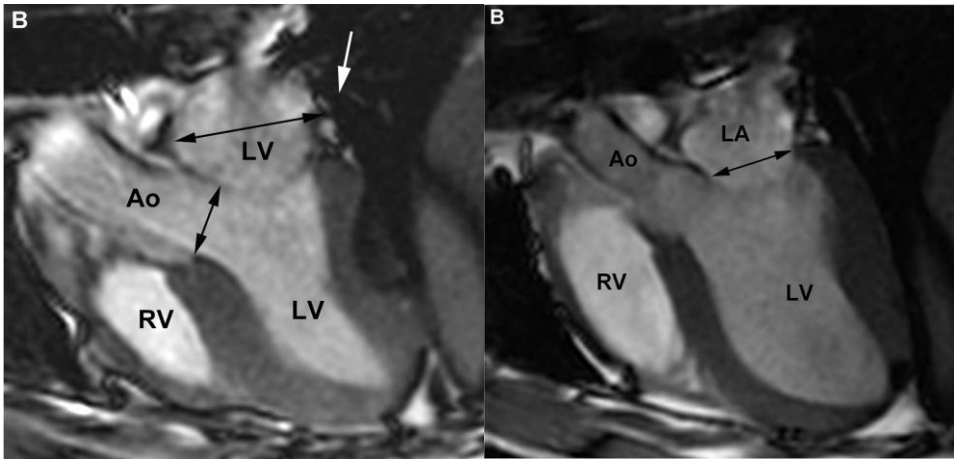

Figure 7: End systolic (left) and end diastolic (right) three-chamber view[4]. Adapted from: Drees, Johnson, Stepien, Munoz Del Rio, Saunders, *et al.* (2015).

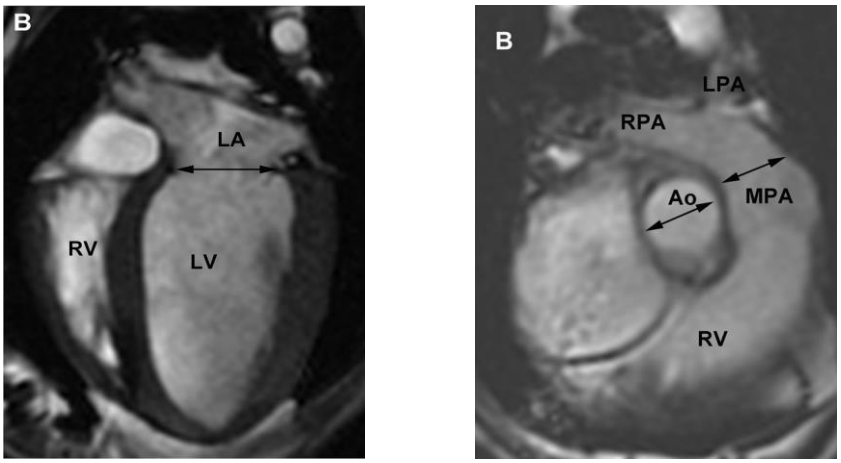

Figure 8: Approximate four-chamber view (left) and transverse plan (right)[5]. Adapted from: Drees, Johnson, Stepien, Munoz Del Rio, Saunders, *et al.* (2015).

In veterinary medicine the use of CMRI has been limited, most likely because of the long examination times, the motion artifacts caused by heart activity and breathing, the need for anaesthesia and the high cost of the examination (Garcia-Rodriguez *et al.*, 2009), these being its major disadvantages. Recently in veterinary medicine, problems due to cardiac and respiratory motion have been overcome through cardiac gating ECG, respiratory navigation and encoding strategies that speed up acquisition times to values compatible with *in vivo* imaging (Gilbert *et al.*, 2010). The major advantage of using

[4] This figure shows measurement of the diameter of the left atrial (right, dark arrow) and aortic annulus (left smallest dark arrow).

[5] These figures show measurement of the mitral annulus diameter (dark arrow) at end diastole (left) and transverse plane view for measurement of the diameter of the proximal aorta (Ao) and the main pulmonary artery (MPA) (right).

Legend: LA, left atrium; LV, left ventricle; RV, right ventricle; Ao, aorta; RPA, right pulmonary artery; LPA, left pulmonary artery.

both high-frequency echocardiography and self-gated CMRI is the reduction of the examination time (Amundsen *et al.*, 2011): this reduction of the anaesthetic time it's very important in geriatric animals and animals with cardiac disease.

2.3. Left ventricular myocardial mass, chamber volume and haemodynamic

CMRI is the non-invasive method of reference for the determination of cardiac mass. Echocardiographic determination of myocardial mass has been based on measurements from two-dimension standard views with extension to three-dimension on the basis of a geometrical model, while contrast MRI allows direct determination of cardiac mass from three-dimension data, providing more accurate mass and volume estimation without relying on any geometric assumptions (Gilbert *et al.*, 2010) (table 2).

Table 2: Right ventricular function variables comparing CMRI, computed tomography and three-dimensional echocardiography in dogs[6]. Adapted from: Kim *et al.* (2013), Sieslack *et al.* (2014) and Meyer *et al.* (2013)

Variable	**CMRI**			**CCT**	**3DE**		**2DE**
	Kim *et al.* (2013)	Meyer *et al.* (2013)	Sieslack *et al.* (2014)	Kim *et al.* (2013)	Meyer *et al.* (2013)	Kim *et al.* (2013)	Sieslack *et al.* (2014)
EDV (ml)	47.73 ± 6.51 (47.46)	37.14 ± 2.69	34.13 ± 1.26	52.75 ± 9.83 (50.05)	32.40 ± 4.15	26.54 ± 6.87 (26.20)	32.88 ± 1.17
ESV (ml)	28.45 ± 7.13 (27.46)	19.68 ± 2.82	16.38 ± 0.92	32.35 ± 9.45 (30.709	15.14 ± 2.30	13.38 ± 4.86 (13.18)	15.05 ± 0.66
SV (ml)	19.27 ± 1.91 (19.50)	-	17.72 ± 0.98	20.38 ± 1.78 (20.15)	-	12.22 ± 2.89 (12.40)	17.92 ± 0.96
EF (%)	41.13 ± 7.21 (40.80)	47.22 ± 4.65	51.92 ± 2.02	39.54 ± 6.04 (41.10)	53.25 ± 2.80	48.87 ± 7.13 (50.25)	53.33 ± 1.69

In a study by MacDonald, Kittleson, *et al.* (2005) on seven domestic cats they observed that the determination of left ventricular mass obtained by CMRI in end-systole was more accurate than echocardiography, with a significantly smaller difference between the measures obtain by CMRI and the measures obtained by echocardiography and true mass of the left ventricle. CMRI derived left ventricular mass closely approximated true left ventricular mass, but echocardiography underestimated true left ventricular mass in six of seven cats of the study, and echocardiography

[6] **Legend:** Mean ± standard deviation values for right ventricular function variables (end-diastolic volume = EDV, end-systolic volume = ESV, stroke volume = SV, ejection fraction = EF) obtained with cardiac magnetic resonance imaging (CMRI), cardiac computed tomography (CCT) and three-dimensional echocardiography (3DE) in 10 healthy anaesthetised beagles (Kim *et al*., 2013), 6 healthy anaesthetised beagles (Sieslack *et al*., 2014) and 10 healthy anaesthetised beagles (Meyer *et al*., 2013).

underestimated left ventricular mass quantified by CMRI in seven of seven cats. They conclude that CMRI using Simpson's rule accurately quantifies left ventricular mass in normal cats and cats with mild left ventricular hypertrophy, and is more accurate and reproducible than the echocardiographic estimate of the same indices. Another recent study by Eskofier *et al.* (2015) shows the same: real-time three-dimensional echocardiography underestimates left ventricular volume in comparison with the gold standard CMRI.

Using steady-state free precession sequences, left ventricular ejection fraction can be calculated; end-diastolic and end-systolic volumes are determined for each section, allowing determination of a global left ventricular ejection fraction using a modification of Simpson's rule. Wall motion can be assessed on short- and long-axis images either qualitatively or quantitatively, focal wall motion abnormalities suggest possible ischemia, whereas global hypokinesis may occur with a nonischemic cardiomyopathy (Jeudy & White, 2008). Roldan-Alzate *et al.* (2014), using the three-directional velocity information, found a strong correlation between: the ratio of the peak tricuspid regurgitation velocity to the flow through the pulmonary arteries, and pulmonary vascular resistance determined at right heart catheterization, in a canine model of acute thromboembolic pulmonary hypertension.

2.4. Valvular heart disease

As mentioned before, echocardiography is the primary non-invasive tool for initial evaluation and longitudinal monitoring of patients with significant valvular heart disease, however echocardiography can be impaired by poor acoustic windows, and is dependent on the skill and experience of the technician (Looi, Kerr, & Gabriel, 2015).

CMRI can provide a comprehensive non-invasive assessment of valvular morphology, quantification of the severity of valvular dysfunction, determination of its aetiology, assessment of the consequences for the heart from the valve lesion including measurement of ventricular volumes and function, evaluation of haemodynamic abnormalities (Looi *et al.*, 2015), measure pulmonary artery flow, tricuspid valve regurgitation velocity, and thereby estimate pulmonary vascular resistance (Abbas *et al.*, 2003). This is a useful adjunct, but is unlikely to replace echocardiography as the first line diagnostic tool for valvular disease in animals with adequate acoustic access (Gilbert *et al.*, 2010). CMRI is reliable for the assessment of regurgitant blood volume and semi-quantitative grading of regurgitated jets and hence for the diagnosis of aortic and mitral regurgitation (Asferg *et al.*, 2012; Gilbert *et al.*, 2010). However, subjective visual assessment of jet properties is of limited value as their characteristics vary depending on CMRI sequences and scanning variables; pressure gradients can be determined and correlate well with echocardiography and catheterisation (Gilbert *et al.*, 2010).

Aortic valve disease can manifest as aortic regurgitation, aortic stenosis or a mixture of both. Structural abnormalities of the valve, congenital or acquired, or disease of the aorta can cause aortic valve disease (Looi *et al.*, 2015). In some diseases, like myxomatous mitral valve disease the advances in CMRI have enabled researcher and clinicians to determine the earliest remodelling

changes that occur (Burchell & Schoeman, 2014). Recently Sargent *et al.* (2015) concluded that, although technically challenging, CMRI is a feasible method to quantify mitral regurgitant fraction in small dogs. To the best of our knowledge there are no reports describing the assessment of valvular disease by CMRI in small animals. The techniques (quantitative flow) should be applicable to clinical veterinary medicine, but may be more challenging in cats due to small cardiac size and faster heart rates. Additionally, the effects of anaesthetic protocols on systolic function may affect valve dynamics (MacDonald *et al.*, 2006).

2.5. Cardiomyopathies

CMRI is well established in the early diagnosis and follow-up of human cardiomyopathies, where it is valuable for both tissue characterisation and assessment of function. Accurate measurement of myocardial mass and function can be used to differentiate physiological and pathological hypertrophy or dilatation (Gilbert *et al.*, 2010). In small animals, one of the strengths of CMRI are the accuracy when measuring myocardial function (Vallee *et al.*, 2004) and tissue morphology (Fattal *et al.*, 2015).

2.5.1. Hypertrophic cardiomyopathy

CMRI has proved to be a useful tool for assessing a hypertrophic heart, especially when echocardiography is inconclusive or suboptimal. This technique allows for a better and more precise characterization of heart volumes and function, tissue morphology (Fattal *et al.*, 2015) and distribution of myocardial hypertrophy (Chun *et al.*, 2010; Fattal *et al.*, 2015), particularly in apical hypertrophic cardiomyopathy (Wigle, 2001). CMRI either makes it possible to exclude other diseases' aetiology that could perhaps mimic hypertrophic cardiomyopathy when assessed by other imaging modalities; CMRI can also detect features related to sudden death, apical aneurysms, and clots, and provides new information for prognosis stratification which helps in treatment planning (Chun *et al.*, 2010).

Currently, it appears that gradient echo CMRI is not useful for measuring diastolic function in cats, the easier and faster method of tissue doppler imaging seems to be a more accurate, less expensive, and also a safer, non-invasive assessment method of diastolic function in cats (MacDonald *et al.*, 2006). In a study by MacDonald, Wisner, et al. (2005) using a family of Main Coon cats with familial hypertrophic cardiomyopathy, contrast enhancement CMRI was not useful for quantification of myocardial fibrosis.

In animals, CMRI was established as an accurate method to quantify the left ventricular mass in cats, and a difference in left ventricular mass can be observed between cats with hypertrophic cardiomyopathy and normal cats (Fattal *et al.*, 2015; MacDonald *et al.*, 2006).

2.5.2. Dilated cardiomyopathy

To the best of our knowledge there are no published studies on dilated cardiomiopathy with CMRI, though based on echocardiographic findings, some diagnosis criteria can be used; CMRI has yet to show advantages over echocardiography in dogs.

2.5.3. Arrhythmogenic Right Ventricular Cardiomyopathy

ARVC is a myocardial disease characterized by fibrofatty replacement of the right ventricular myocardium and ventricular tachyarrhythmia being reported most commonly in the Boxer dog. Although ARVC is characterized as a myocardial disease and the impact of the disease on the function of the right ventricle has not been well studied (Baumwart *et al.*, 2009). A spin echo technique allows for the identification of the characteristic high signal intensity associated with fat infiltration, diffuse and focal thinning (figure 9), focal aneurysms and systolic and diastolic dysfunction. Fat suppression techniques can be used in order to diminish the high fat signal and confirm fatty infiltration (Constantine *et al.*, 2004).

Baumwart *et al.* (2009) found an abnormal global right ventricular systolic function and little to no morphological changes in dogs with ARVC compared with healthy control dogs. The observation of abnormal right ventricular function is consistent with the presence of a myocardial disease but has not been previously demonstrated in Boxers with ARVC because of the difficulty in imaging and assessing the right ventricle. The findings observed in that study are similar to human CMRI studies of young individuals with mild ARVC. Supporting the close resemblance of the canine disease and human ARVC, both diseases share a profile of sudden death, ventricular arrhythmias of probable right ventricular origin, syncope, right ventricular chamber enlargement, aneurysm, right ventricular myocyte loss, fatty replacement, myocarditis and apoptosis, Basso *et al.* (2004) proposed Boxer ARVC as a new animal model for human ARVC. These authors concluded that *in vivo* CMRI should allow for the diagnosis of the condition and the assessment of its progression. In the same study, all 14 hearts with ARVC displayed high transmural signal intensity in the anterolateral and/or infundibular regions of the right, corresponding anatomically to those areas of right ventricle where fat was identified by histopathology.

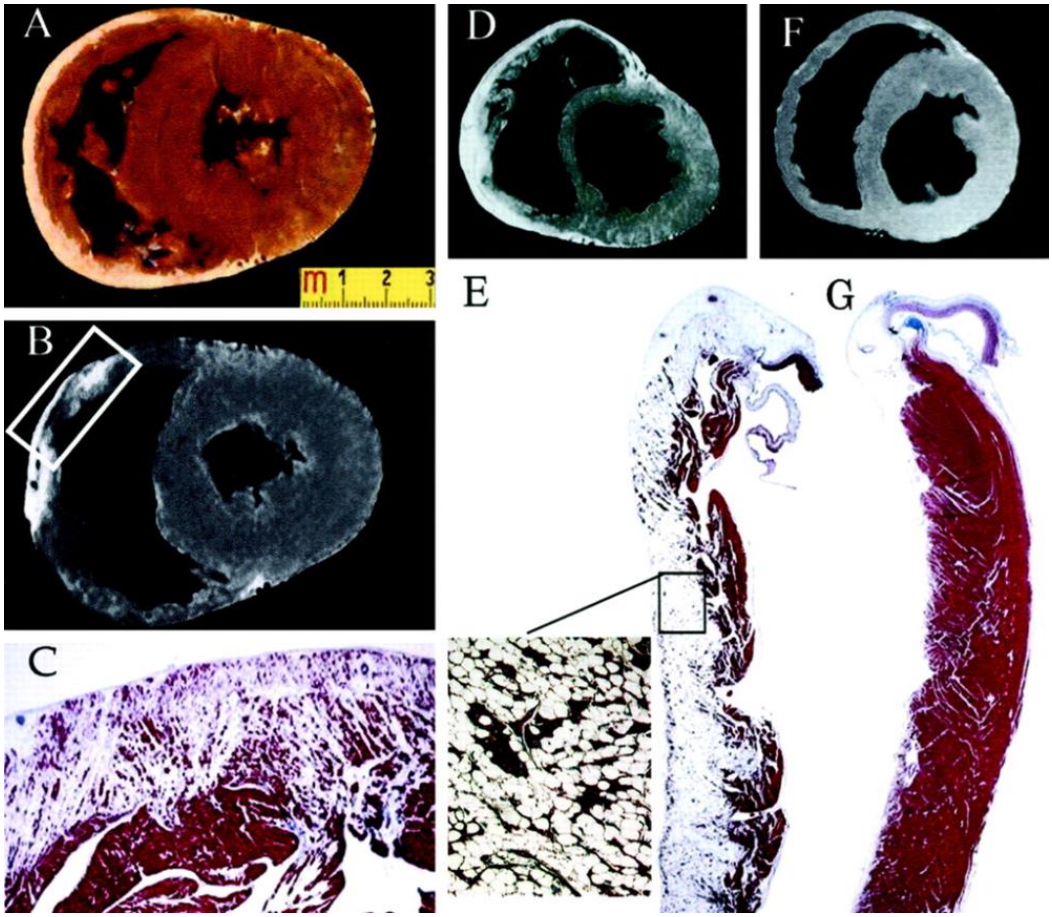

Figure 9: Pathological changes in boxer dogs with ARVC[7]. Source: Basso *et al.* (2004).

2.5.4. Myocarditis and myocardial viability

Currently, CMRI is the preferred non-invasive imaging tool in the workup of myocarditis in humans (Rinkevich-Shop *et al.*, 2013), CMRI is being used in ischemic and nonischemic myocardial disease to assess myocardial perfusion, viability (Jeudy & White, 2008) and infarct size (Amado *et al.*, 2004). Rinkevich-Shop *et al.* (2013) found that CMRI accurately identified the location and the extent of myocardial damage, which corresponded with the histopathology of myocarditis and detected regional and global left ventricular dysfunction and an increase in wall thickness that most likely reflects inflammation and oedema (figure 10).

[7] A, B, and C are from a boxer dog with ventricular tachycardia and sudden death during physical activity. A, Gross heart specimen cut in cross section. B, T1-weighted post-mortem MRI corresponding to same cross-sectional plane as shown in A, presenting dilatation of right ventricle cavity however the wall thickness is normal. C, histopathological section of right ventricle wall from region of bright MRI signals (delineated by the box in B); this histological preparation shows marked transmural fatty replacement. D and E are from other boxer dog with ventricular tachycardia and congestive heart failure. D, Cross-sectional MRI image shows bright, high-intensity signal in right ventricle infundibulum. E, Panoramic histopathological section from region of bright MRI signals demonstrating massive, diffuse fatty replacement of atrophic myocardium. Inset shows small islands of a few surviving myocytes surrounded by fat. F and G are from a normal control dog. F, Cross-sectional MRI showing absence of bright MRI signals in RV wall. G, Panoramic histopathological section demonstrates normal right ventricle myocardial architecture, from a healthy dog.

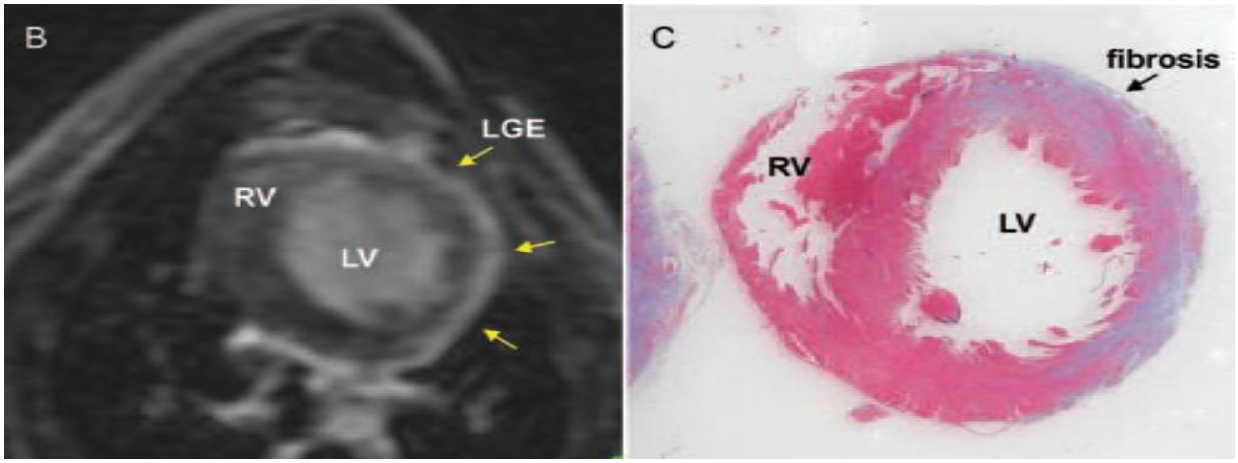

Figure 10: Late gadolinium enhanced (LGE) distribution in left ventricle (LV) of rats with myocarditis[8]. Image courtesy of Rinkevich-Shop *et al.* (2013).

2.6. Congenital heart disease

Diagnosis of extracardiac intrathoracic vascular anomalies is of clinical importance but remains challenging. Traditional imaging modalities, such as radiography, echocardiography, and angiography, are inherently limited by the difficulties of a two-dimension approach to a three-dimensio object (Henjes, Nolte, & Wefstaedt, 2011). Recently, MRI has been introduced as a cardiac diagnostic tool and has gained increasing importance in the non-invasive examination of congenital heart defects in humans (Garcia-Rodriguez *et al.*, 2009; Sieslack *et al.*, 2014), playing a key role in the diagnostic of infantile congenital heart disease, even in complicated cases (Garcia-Rodriguez *et al.*, 2009; Gilbert *et al.*, 2010).

Another study by Lopez-Alvarez *et al.* (2011) showed that echocardiography did not identify an aberrant vessel entering the caudal right atrium, apart from the coronary sinus. Also, the echocontrast study was negative (as no contrast was detected in the caudal right atrium). However, CMRI showed that the coronary sinus and caudal vena cava converged into the caudal right atrium. This negative echocontrast study may be the consequence of insufficient contrast administered, but was most likely due to the large derivation of the flow to the azygous vein, with contrast arriving in the cranial right atrium, indicating disruption of caudal venous caval flow to the heart.

Ranjan *et al.* (2014) used MRI and magnetic resonance angiography to further characterize a rare venous anomaly in a goat, the persistent left cranial vena cava. This is the first report including MRI and magnetic resonance angiography characterization of persistent left cranial vena cava and prominent coronary sinus with successful cardiac pacemaker implantation using the persistent left cranial vena cava. Contrast-enhanced magnetic resonance angiography offers an additional non-invasive method of patent ductus arteriosus examination especially when transthoracic

[8] (B) The short-axis view of representative late gadolinium enhanced images of a rat heart with typical epicardial late gadolinium enhanced (white strip, yellow arrows). (C) Equivalent heart section shows a high correlation in the location of fibrosis between histopathology and CMRI.

echocardiography is unable to provide precise measurements of the duct and most importantly from the moment that an interventional procedure is anticipated. The wide field of view, multiplanar imaging and the ability to reconstruct complicated anatomical information in three-dimensional are all valuable attributes of magnetic resonance angiography (Louvet *et al.*, 2010).

2.7. Ischemic disease

Imaging of human ischaemic heart disease including the coronary arteries, coronary flow and myocardial viability is of increasing importance in human medicine, but is unlikely to be important in clinical veterinary medicine (Gilbert *et al.*, 2010).

In animal experiments, excellent agreement between the extent of hyperenhancement on contrast-enhanced MRI and the histologically determined infarct size was demonstrated. The major advantage of contrast-enhanced MRI is superior spatial resolution, which allows differentiation between transmural necrosis and subendocardial necrosis (Schinkel, Poldermans, Elhendy, & Bax, 2007), as was confirmed by Rinkevich-Shop *et al.* (2013). A paramagnetic contrast agent, gadolinium meglumine, is administered intravenously and becomes distributed in the extracellular space before reabsorption by the myocardial capillary bed (and final excretion via the kidneys). In abnormal myocardial fibrosis, the extracellular space is expanded resulting in pooling of the contrast agent with slow washout. This appears as hyperintense bright areas on T1-weighted gradient echo images – a phenomenon known as '*delayed enhancement*'(Gilbert *et al.*, 2010).

Thajudeen *et al.* (2015) demonstrated that the high-resolution mapping system and the multielectrode catheter accurately localize ventricular scar and abnormal myocardial tissue in an experimental canine infarct model. The system helps to rapidly map and identify abnormal electrocardiograms and delineates the presence, location and timing of isolated late potentials. Using the high-resolution bipolar and unipolar voltage maps may allow to differentiate between scar types and degree of transmurality.

2.8. Pericardial disease

CMRI is widely applied in human medicine in the imaging of pericardial disease, and this is likely to be in the same way applicable to dogs and cats (Gilbert *et al.*, 2010). CMRI also has the potential to yield clinically relevant information in many cases of canine pleural and pericardial effusion (Boddy *et al.*, 2011).

In a recent study to differentiate benign and neoplastic causes of pleural effusion, performed by Boddy *et al.* (2011) CMRI did not substantially improve diagnosis of cardiac tumours compared with transthoracic echocardiography in the cases on the study, but it yielded useful descriptive information regarding extent, anatomic location, and potential tumour type and confirmed that CMRI requires extensive additional training for tumour identification.

2.9. Other applications

A current development in human clinical practice is interventional CMRI – the application of CMRI as an imaging modality in interventional cardiology (Gilbert *et al.*, 2010) as an alternative real-time technique to conventional fluoroscopy (Constantine *et al.*, 2004). CMRI has inherent advantages over fluoroscopy in interventional imaging: it is three-dimensional, has better soft tissue contrast, provides pathological information, and does not expose the operator and subject to ionising radiation (Gilbert *et al.*, 2010). In 2014 Markovic *et al.* (2014) showed the utility of multiple imaging modalities for assessment of anomalies of the ascending aorta, main pulmonary artery, and dissecting main pulmonary artery aneurysms. This information is particularly useful in planning surgical treatment of these disorders. Even though CMRI has shown to be reliable and accurate in human cardiology diagnosis, the need for general anaesthesia, CMRI compatible monitoring equipment and the time required for a CMRI study means it is not likely to be a first line tool in small animal the near future (Lopez-Alvarez *et al.*, 2011; MacDonald, Kittleson, *et al.*, 2005).

3. Specific difficulties with transposition of human Cardiac Magnetic Resonance Imaging to veterinary cardiology

The vast majority of the existing studies are human clinical studies and experimental small rodent studies, hence the need for more research in veterinary medicine.

4. Cardiac Magnetic Resonance Imaging studies in cats and dogs – experimental or clinical?

MRI was adopted slowly by veterinary schools because of the expense and uncertainty about its real life applications in animals (Constantine *et al.*, 2004; Gilbert *et al.*, 2010). Initially, MRI was considered mainly as a research tool, and relatively few clinical studies were performed. However, with the increasing numbers of veterinary specialists and referral practices, greater public awareness of MRI, decreasing operating costs of MRI units, and – in some countries – increased popularity of veterinary health insurances, veterinary MRI has become increasingly available. The growing tendency is for veterinary schools and referral practices to install MRI systems for their exclusive use (Constantine *et al.*, 2004; Gavin, 2011).

5. Future perspectives

Future use and clinical utility of CMRI in the evaluation of small animal patients with congenital or acquired cardiac disease has being assessed in recent studies (Drees, Johnson, Stepien, Munoz Del Rio, & Francois, 2015). Other emerging techniques based on MRI, is cardiac magnetic resonance elastography (this is a novel imaging technique to noninvasively quantify myocardial stiffness) (da Silveira *et al.*, 2014), and magnetic resonance angiography (Contreras *et al.*, 2008).

A methodology for the simulation of heart function that combines an MRI-based model of cardiac electromechanics with a Navier–Stokes-based hemodynamic model is in development. This technique accurately describes ventricular geometry and fiber orientation (Choi, Constantino, Vedula, Trayanova, & Mittal, 2015).

Conclusion

CMRI has a strong potential for cardiac imaging in small animals (Vallee *et al.*, 2004). MRI technology will surely continue to develop and magnetic resonance scanners will become more readily available to the veterinary *curricula*, requiring more teaching and training on this subject in veterinary *curricula* and at postgraduate level; veterinary radiologists must develop and participate in educational programs in MRI, in order to optimally support colleagues in first opinion and referral practices who need guidance selecting patients for MRI, and help interpreting magnetic resonance scans (Gavin, 2011). MRI is an alternative to many existing imaging modalities and veterinarians must take decisions concerning its benefits on their patients. It is important that these choices are made according to evidence acquired from well-designed studies of diagnostic performance and clinical impact (Gavin, 2011).

CMRI is still an emerging technique and has become an important diagnostic methodology in human clinical cardiology. Echocardiography will not be replaced by CMRI but this offers distinct advantages in imaging when three-dimensional organisation of the vasculature is required, when precise volume measurements are needed or when myocardial characterisation is indicated (Gilbert *et al.*, 2010). The main generic advantages of CMRI include a wide field-of-view, absence of ionizing radiation, a variety of imaging sequences to optimize contrast and highlight specific structures, and for some applications, avoidance of intravenous contrast medium (Constantine *et al.*, 2004; Jeudy & White, 2008). One of the major disadvantages of CMRI and other magnetic resonance techniques has been the need to anaesthetize the animal for the examinations (Sieslack, Dziallas, Nolte, & Wefstaedt, 2013). In comparison with echocardiography, CMRI provides a better understanding of the anatomy of intra- or para-cardiac abnormalities. A recent study in dogs suggest that echocardiography is a good technique for detecting heart base tumours, but CMRI provides a better assessment of the exact relationship of the tumour with the surrounding great vessels and general hemodynamic consequences, such as alternate venous return through the azygos vein (Mai, Weisse, & Sleeper, 2010). CMRI also provides improved resolution and better soft tissue contrast (Sparrow *et al.*, 2005).

Advanced techniques like perfusion imaging, delayed enhancement or tag imaging look promising, but an effort is still needed to standardize the acquisition protocols and data analysis (Vallee *et al.*, 2004). More recently, veterinary clinical studies have validated left ventricular mass determination by CMRI as an effective diagnostic and clinical research tool, and '*delayed enhancement'* techniques have shown promising results. Diastolic function assessment by CMRI has been proven to be useful in the cat thus far, but this should be investigated in further studies (Gilbert *et al.*, 2010).

In conclusion, we can affirm that CMRI is a well developed and useful diagnostic tool in human cardiology. In small animal cardiology it poses some additional obstacles that impair its feasibility, mainly the need for general anaesthesia of the patient and relative cost of the technique for the owner. Also, it is a technique with a relatively difficult learning curve and maintenance costs. We hope that in the near future these obstacles can be overcome and this technique can be made widely available for veterinary patients worldwide.

References

Abbas, A. E., Fortuin, F. D., Schiller, N. B., Appleton, C. P., Moreno, C. A., & Lester, S. J. (2003). A simple method for noninvasive estimation of pulmonary vascular resistance. *J Am Coll Cardiol, 41*(6), 1021-1027. doi: 10.1016/S0735-1097(02)02973-X

Amado, L. C., Gerber, B. L., Gupta, S. N., Rettmann, D. W., Szarf, G., Schock, R., Nasir, K., Kraitchman & D. L., Lima, J. A. (2004). Accurate and objective infarct sizing by contrast-enhanced magnetic resonance imaging in a canine myocardial infarction model. *J Am Coll Cardiol, 44*(12), 2383-2389. doi: 10.1016/j.jacc.2004.09.020

Amundsen, B. H., Ericsson, M., Seland, J. G., Pavlin, T., Ellingsen, O., & Brekken, C. (2011). A comparison of retrospectively self-gated magnetic resonance imaging and high-frequency echocardiography for characterization of left ventricular function in mice. *Lab Anim, 45*(1), 31-37. doi: 10.1258/la.2010.010094

Asferg, C., Usinger, L., Kristensen, T. S., & Abdulla, J. (2012). Accuracy of multi-slice computed tomography for measurement of left ventricular ejection fraction compared with cardiac magnetic resonance imaging and two-dimensional transthoracic echocardiography: a systematic review and meta-analysis. *Eur J Radiol, 81*(5), e757-762. doi: 10.1016/j.ejrad.2012.02.002

Basso, C., Fox, P. R., Meurs, K. M., Towbin, J. A., Spier, A. W., Calabrese, F., Maron, B. J. & Thiene, G. (2004). Arrhythmogenic right ventricular cardiomyopathy causing sudden cardiac death in boxer dogs: a new animal model of human disease. *Circulation, 109*(9), 1180-1185. doi: 10.1161/01.CIR.0000118494.07530.65

Baumwart, R. D., Meurs, K. M., & Raman, S. V. (2009). Magnetic resonance imaging of right ventricular morphology and function in boxer dogs with arrhythmogenic right ventricular cardiomyopathy. *J Vet Intern Med, 23*(2), 271-274. doi: 10.1111/j.1939-1676.2008.0266.x

Boddy, K. N., Sleeper, M. M., Sammarco, C. D., Weisse, C., Ghods, S., & Litt, H. I. (2011). Cardiac magnetic resonance in the differentiation of neoplastic and nonneoplastic pericardial effusion. *J Vet Intern Med, 25*(5), 1003-1009. doi: 10.1111/j.1939-1676.2011.0762.x

Burchell, R. K., & Schoeman, J. (2014). Advances in the understanding of the pathogenesis, progression and diagnosis of myxomatous mitral valve disease in dogs. *J S Afr Vet Assoc, 85*(1), 1101. doi: 10.4102/jsava.v85i1.1101

Choi, Y. J., Constantino, J., Vedula, V., Trayanova, N., & Mittal, R. (2015). A New MRI-Based Model of Heart Function with Coupled Hemodynamics and Application to Normal and Diseased Canine Left Ventricles. *Front Bioeng Biotechnol, 3*, 140. doi: 10.3389/fbioe.2015.00140

Chun, E. J., Choi, S. I., Jin, K. N., Kwag, H. J., Kim, Y. J., Choi, B. W., Lee W. & Park, J. H. (2010). Hypertrophic cardiomyopathy: assessment with MR imaging and multidetector CT. *Radiographics, 30*(5), 1309-1328. doi: 10.1148/rg.305095074

Constantine, G., Shan, K., Flamm, S. D., & Sivananthan, M. U. (2004). Role of MRI in clinical cardiology. *Lancet, 363*(9427), 2162-2171. doi: 10.1016/S0140-6736(04)16509-4

Contreras, S., Vazquez, J. M., Miguel, A. D., Morales, M., Gil, F., Lopez, O., & Arencibia, A. (2008). Magnetic resonance angiography of the normal canine heart and associated blood vessels. *Vet J, 178*(1), 130-132. doi: 10.1016/j.tvjl.2007.06.027

da Silveira, J., Scansen, B. A., Wassenaar, P. A., Raterman, B., Jin, N., White, R. D. & Bonagura J. D., Kolipaka, A. (2014). MR elastography-derived right ventricular myocardial stiffness in dogs with congenital pulmonary valve stenosis: correlation with myocardial relaxation times and ECV. *Journal of Cardiovascular Magnetic Resonance, 16*(Suppl 1), P82. doi: 10.1186/1532-429x-16-s1-p82

Dorosz, J. L., Lezotte, D. C., Weitzenkamp, D. A., Allen, L. A., & Salcedo, E. E. (2012). Performance of 3-dimensional echocardiography in measuring left ventricular volumes and ejection fraction:

a systematic review and meta-analysis. *J Am Coll Cardiol, 59*(20), 1799-1808. doi: 10.1016/j.jacc.2012.01.037

Drees, R., Johnson, R. A., Stepien, R. L., Munoz Del Rio, A., & Francois, C. J. (2015). Effects of two different anesthetic protocols on cardiac flow measured by two dimensional phase contrast magnetic resonance imaging. *Vet Radiol Ultrasound, 56*(2), 168-175. doi: 10.1111/vru.12200

Drees, R., Johnson, R. A., Stepien, R. L., Munoz Del Rio, A., Saunders, J. H., & Francois, C. J. (2015). Quantitative Planar and Volumetric Cardiac Measurements Using 64 Mdct and 3t Mri Vs. Standard 2d and M-Mode Echocardiography: Does Anesthetic Protocol Matter? *Vet Radiol Ultrasound, 56*(6), 638-657. doi: 10.1111/vru.12269

Eskofier, J., Wefstaedt, P., Beyerbach, M., Nolte, I., & Hungerbuhler, S. O. (2015). Quantification of left ventricular volumes and function in anesthetized beagles using real-time three-dimensional echocardiography: 4D-TomTec analysis versus 4D-AutLVQ analysis in comparison with cardiac magnetic resonance imaging. *BMC Vet Res, 11*(1), 260. doi: 10.1186/s12917-015-0568-5

Fattal, J., Henry, M. A., Ou, S., Bradette, S., Papas, K., Marcotte, F., Garceau P. & Pressacco, J. (2015). Magnetic resonance imaging of hypertrophic cardiomyopathy: beyond left ventricular wall thickness. *Can Assoc Radiol J, 66*(1), 71-78. doi: 10.1016/j.carj.2014.07.005

Garcia-Rodriguez, M. B., Granja, M. A., Garcia, C. C., Gonzalo Orden, J. M., Cano Rabano, M. J., & Prieto, I. D. (2009). Complex cardiac congenital defects in an adult dog: an ultrasonographic and magnetic resonance imaging study. *Can Vet J, 50*(9), 933-935.

Gavin, P. R. (2011). Growth of clinical veterinary magnetic resonance imaging. *Vet Radiol Ultrasound, 52*(1 Suppl 1), S2-4. doi: 10.1111/j.1740-8261.2010.01779.x

Gilbert, S. H., McConnell, F. J., Holden, A. V., Sivananthan, M. U., & Dukes-McEwan, J. (2010). The potential role of MRI in veterinary clinical cardiology. *Vet J, 183*(2), 124-134. doi: 10.1016/j.tvjl.2008.11.018

Hao, D., Ai, T., Goerner, F., Hu, X., Runge, V. M., & Tweedle, M. (2012). MRI contrast agents: basic chemistry and safety. *J Magn Reson Imaging, 36*(5), 1060-1071. doi: 10.1002/jmri.23725

Henjes, C. R., Nolte, I., & Wefstaedt, P. (2011). Multidetector-row computed tomography of thoracic aortic anomalies in dogs and cats: patent ductus arteriosus and vascular rings. *BMC Vet Res, 7*, 57. doi: 10.1186/1746-6148-7-57

Jeudy, J., & White, C. S. (2008). Cardiac magnetic resonance imaging: techniques and principles. *Semin Roentgenol, 43*(3), 173-182. doi: 10.1053/j.ro.2008.02.003

Kali, A., Cokic, I., Tang, R. L., Yang, H. J., Sharif, B., Marban, E., Li, D., Berman, D. S., & Dharmakumar, R. (2014). Determination of location, size, and transmurality of chronic myocardial infarction without exogenous contrast media by using cardiac magnetic resonance imaging at 3 T. *Circ Cardiovasc Imaging, 7*(3), 471-481. doi: 10.1161/CIRCIMAGING.113.001541

Kim, J. H., Lee, M. S., Lee, S. Y., Kim, S. Y., Lee, S. J., Park, Y. W., Yeo, J. H., Song, S. H., Park, N. W., Hong, S. W., Choi, S. I. & Eom, K. D. (2013). Contrast echocardiography to assess left ventricular volume and function in Beagle dogs: comparison with 3-Tesla dual source parallel cardiac magnetic resonance imaging. *Vet J, 198*(2), 450-456. doi: 10.1016/j.tvjl.2013.08.007

Looi, J. L., Kerr, A. J., & Gabriel, R. (2015). Morphology of congenital and acquired aortic valve disease by cardiovascular magnetic resonance imaging. *Eur J Radiol, 84*(11), 2144-2154. doi: 10.1016/j.ejrad.2015.07.022

Lopez-Alvarez, J., Dukes-McEwan, J., Martin, M. W., Killick, D., Fonfara, S., & Fraser McConnell, J. (2011). Balloon dilation of an imperforate cor triatriatum dexter in a Golden Retriever with concurrent double-chambered right ventricle and subsequent evaluation by cardiac magnetic resonance imaging. *J Vet Cardiol, 13*(3), 211-218. doi: 10.1016/j.jvc.2011.04.004

Louvet, A., Duconseille, A. C., & Lazard, P. (2010). Contrast-enhanced magnetic resonance angiography of patent ductus arteriosus in a dog. *J Small Anim Pract, 51*(8), 451-453. doi: 10.1111/j.1748-5827.2010.00970.x

MacDonald, K. A., Kittleson, M. D., Garcia-Nolen, T., Larson, R. F., & Wisner, E. R. (2006). Tissue Doppler imaging and gradient echo cardiac magnetic resonance imaging in normal cats and cats with hypertrophic cardiomyopathy. *J Vet Intern Med, 20*(3), 627-634. doi: 0891-6640/06/2003-0024/$3.00/0

MacDonald, K. A., Kittleson, M. D., Reed, T., Larson, R., Kass, P., & Wisner, E. R. (2005). Quantification of left ventricular mass using cardiac magnetic resonance imaging compared with echocardiography in domestic cats. *Vet Radiol Ultrasound, 46*(3), 192-199. doi: 10.1111/j.1740-8261.2005.00038.x

MacDonald, K. A., Wisner, E. R., Larson, R. F., Klose, T., Kass, P. H., & Kittleson, M. D. (2005). Comparison of myocardial contrast enhancement via cardiac magnetic resonance imaging in healthy cats and cats with hypertrophic cardiomyopathy. *Am J Vet Res, 66*(11), 1891-1894.

Mai, W., Badea, C. T., Wheeler, C. T., Hedlund, L. W., & Johnson, G. A. (2005). Effects of breathing and cardiac motion on spatial resolution in the microscopic imaging of rodents. *Magn Reson Med, 53*(4), 858-865. doi: 10.1002/mrm.20400

Mai, W., Weisse, C., & Sleeper, M. M. (2010). Cardiac magnetic resonance imaging in normal dogs and two dogs with heart base tumor. *Vet Radiol Ultrasound, 51*(4), 428-435.

Markovic, L. E., Kellihan, H. B., Roldan-Alzate, A., Drees, R., Bjorling, D. E., & Francois, C. J. (2014). Advanced multimodality imaging of an anomalous vessel between the ascending aorta and main pulmonary artery in a dog. *J Vet Cardiol, 16*(1), 59-65. doi: 10.1016/j.jvc.2013.12.002

Meyer, J., Wefstaedt, P., Dziallas, P., Beyerbach, M., Nolte, I., & Hungerbuhler, S. O. (2013). Assessment of left ventricular volumes by use of one-, two-, and three-dimensional echocardiography versus magnetic resonance imaging in healthy dogs. *Am J Vet Res, 74*(9), 1223-1230. doi: 10.2460/ajvr.74.9.1223

Moon, J. C., Reed, E., Sheppard, M. N., Elkington, A. G., Ho, S. Y., Burke, M., . . . Pennell, D. J. (2004). The histologic basis of late gadolinium enhancement cardiovascular magnetic resonance in hypertrophic cardiomyopathy. *J Am Coll Cardiol, 43*(12), 2260-2264. doi: 10.1016/j.jacc.2004.03.035

Mor-Avi, V., Jenkins, C., Kuhl, H. P., Nesser, H. J., Marwick, T., Franke, A., Ebner, C., Freed, B. H., Steringer-Mascherbauer, R., Pollard, H., Weinert, L., Niel, J., Sugeng, L. & Lang, R. M. (2008). Real-time 3-dimensional echocardiographic quantification of left ventricular volumes: multicenter study for validation with magnetic resonance imaging and investigation of sources of error. *JACC Cardiovasc Imaging, 1*(4), 413-423. doi: 10.1016/j.jcmg.2008.02.009

Odegard, K. C., DiNardo, J. A., Tsai-Goodman, B., Powell, A. J., Geva, T., & Laussen, P. C. (2004). Anaesthesia considerations for cardiac MRI in infants and small children. *Paediatr Anaesth, 14*(6), 471-476. doi: 10.1111/j.1460-9592.2004.01221.x

Puntmann, V. O., Gebker, R., Duckett, S., Mirelis, J., Schnackenburg, B., Graefe, M., . . . Nagel, E. (2013). Left ventricular chamber dimensions and wall thickness by cardiovascular magnetic resonance: comparison with transthoracic echocardiography. *Eur Heart J Cardiovasc Imaging, 14*(3), 240-246. doi: 10.1093/ehjci/jes145

Ranjan, R., Dosdall, D., Norlund, L., Higuchi, K., Silvernagel, J. M., Olsen, A. L., Razavi, R., Fleck, E & Marrouche, N. F. (2014). Diagnostic imaging and pacemaker implantation in a domestic goat with persistent left cranial vena cava. *J Vet Cardiol, 16*(1), 45-50. doi: 10.1016/j.jvc.2013.11.001

Rinkevich-Shop, S., Konen, E., Kushnir, T., Epstein, F. H., Landa-Rouben, N., Goitein, O., Ben Mordechai, T., Feinberg, M. S., Afek, A. & Leor, J. (2013). Non-invasive assessment of experimental autoimmune myocarditis in rats using a 3 T clinical MRI scanner. *Eur Heart J Cardiovasc Imaging, 14*(11), 1069-1079. doi: 10.1093/ehjci/jet044

Roldan-Alzate, A., Frydrychowicz, A., Johnson, K. M., Kellihan, H., Chesler, N. C., Wieben, O., & Francois, C. J. (2014). Non-invasive assessment of cardiac function and pulmonary vascular resistance in an canine model of acute thromboembolic pulmonary hypertension using 4D

flow cardiovascular magnetic resonance. *J Cardiovasc Magn Reson, 16*, 23. doi: 10.1186/1532-429X-16-23

Sargent, J., Connolly, D. J., Watts, V., Motskula, P., Volk, H. A., Lamb, C. R., & Fuentes, V. L. (2015). Assessment of mitral regurgitation in dogs: comparison of results of echocardiography with magnetic resonance imaging. *J Small Anim Pract, 56*(11), 641-650. doi: 10.1111/jsap.12410

Schinkel, A. F., Poldermans, D., Elhendy, A., & Bax, J. J. (2007). Assessment of myocardial viability in patients with heart failure. *J Nucl Med, 48*(7), 1135-1146. doi: 10.2967/jnumed.106.038851

Sharpley, J., Thode, H., Sestina, L., Park, R., Monnet, E., & Kraft, S. L. (2009). Distal abdominal aortic thrombosis diagnosed by three-dimensional contrast-enhanced magnetic resonance angiography. *Vet Radiol Ultrasound, 50*(4), 370-375. doi: 10.1111/j.1740-8261.2009.01552.x

Sieslack, A. K., Dziallas, P., Nolte, I., & Wefstaedt, P. (2013). Comparative assessment of left ventricular function variables determined via cardiac computed tomography and cardiac magnetic resonance imaging in dogs. *Am J Vet Res, 74*(7), 990-998. doi: 10.2460/ajvr.74.7.990

Sieslack, A. K., Dziallas, P., Nolte, I., Wefstaedt, P., & Hungerbuhler, S. O. (2014). Quantification of right ventricular volume in dogs: a comparative study between three-dimensional echocardiography and computed tomography with the reference method magnetic resonance imaging. *BMC Vet Res, 10*, 242. doi: 10.1186/s12917-014-0242-3

Sparrow, P. J., Kurian, J. B., Jones, T. R., & Sivananthan, M. U. (2005). MR imaging of cardiac tumors. *Radiographics, 25*(5), 1255-1276. doi: 10.1148/rg.255045721

Sugimoto, K., Fujii, Y., Sunahara, H., & Aoki, T. (2015). Assessment of left ventricular longitudinal function in cats with subclinical hypertrophic cardiomyopathy using tissue Doppler imaging and speckle tracking echocardiography. *J Vet Med Sci, 77*(9), 1101-1108. doi: 10.1292/jvms.14-0354

Thajudeen, A., Jackman, W. M., Stewart, B., Cokic, I., Nakagawa, H., Shehata, M., Amorn, A. M., Kali, A., Liu, E., Harlev, D., Bennett, N., Dharmakumar, R., Chugh, S. & S.Wang, X. (2015). Correlation of scar in cardiac MRI and high-resolution contact mapping of left ventricle in a chronic infarct model. *Pacing Clin Electrophysiol, 38*(6), 663-674. doi: 10.1111/pace.12581

Vallee, J. P., Ivancevic, M. K., Nguyen, D., Morel, D. R., & Jaconi, M. (2004). Current status of cardiac MRI in small animals. *MAGMA, 17*(3-6), 149-156. doi: 10.1007/s10334-004-0066-4

Wigle, E. D. (2001). Cardiomyopathy: The diagnosis of hypertrophic cardiomyopathy. *Heart, 86*(6), 709-714.